Ralphcannonite, $AgZn_2TlAs_2S_6$, a new mineral of the routhierite isotypic series from Lengenbach, Binn Valley, Switzerland

LUCA BINDI[1*], CRISTIAN BIAGIONI[2], THOMAS RABER[3], PHILIPPE ROTH[4], FABRIZIO NESTOLA[5]

[1] *Dipartimento di Scienze della Terra, Università degli Studi di Firenze, Via G. La Pira, 4, I-50121 Firenze, Italy*
[2] *Dipartimento di Scienze della Terra, Università di Pisa, Via Santa Maria, 53, I-56126 Pisa, Italy*
[3] *FGL (Forschungsgemeinschaft Lengenbach), Edith-Stein-Str. 9, D-79110 Freiburg, Germany*
[4] *FGL (Forschungsgemeinschaft Lengenbach), Ilanzhofweg 2, CH-8057 Zurich, Switzerland*
[5] *Dipartimento di Geoscienze, Università di Padova, Via Gradenigo, 6, I-35131 Padova, Italy*

**e-mail address*: luca.bindi@unifi.it

ABSTRACT

The new mineral species ralphcannonite, $AgZn_2TlAs_2S_6$, was discovered in the Lengenbach quarry, Binn Valley, Wallis, Switzerland. It occurs as metallic black equant, isometric to prismatic crystals, up to 50 μm, associated with dufrénoysite, hatchite, realgar, and baryte. Minimum and maximum reflectance data for COM wavelengths in air are [λ (nm): *R* (%)]: 471.1: 25.8/27.1; 548.3: 25.2/26.6; 586.6: 24.6/25.8; 652.3: 23.9/24.8. Electron microprobe analyses give (wt%): Cu 2.01(6), Ag 8.50(16), Zn 10.94(20), Fe 3.25(8), Hg 7.92(12), Tl 24.58(26), As 18.36(19), Sb 0.17(4), S 24.03(21), total 99.76(71). On the basis of 12 atoms per formula unit, the chemical formula of ralphcannonite is $Ag_{0.63(2)}Cu_{0.25(2)}Zn_{1.35(5)}Fe_{0.47(1)}Hg_{0.32(2)}Tl_{0.97(3)}[As_{1.97(6)}Sb_{0.01(1)}]_{\Sigma 1.98(5)}S_{6.03(8)}$. The new mineral is tetragonal, space group $I\bar{4}2m$, with *a* 9.861(2), *c* 11.125(3) Å, *V* 1081.8(4) Å^3, *Z* = 4. Main diffraction lines of the calculated powder diagram are [*d*(in Å), intensity, *hkl*]: 4.100, 85, 211; 3.471, 40, 103; 2.954, 100, 222; 2.465, 24, 400; 2.460, 39, 303. The crystal structure of ralphcannonite has been refined by X-ray single-crystal data to a final $R_1 = 0.030$, on the basis of 140 observed reflections. It shows a three dimensional framework of (Ag,Zn)-centered tetrahedra (1 *M*1 + 2 *M*2), with channels parallel to [001] hosting TlS_6 and $(As,Sb)S_3$ disymmetric polyhedra. Ralphcannonite is derived from its isotype routhierite $^{M1}Cu^{M2}Hg_2TlAs_2S_6$ through the double heterovalent substitution $^{M1}Cu^{+} + {}^{M2}Hg^{2+} \rightarrow {}^{M1}Zn^{2+} + {}^{M2}Ag^{+}$. This substitution obeys a steric constraint, with Ag^{+}, the largest cation relative to Zn^{2+} and Cu^{+}, entering the largest *M*2 site, as observed in arsiccioite. The ideal crystal-chemical formula of ralphcannonite is $^{M1}Zn^{M2}(Zn_{0.5}Ag_{0.5})_2TlAs_2S_6$.

Keywords: ralphcannonite, new mineral species, sulfosalt, thallium, zinc, silver, arsenic, crystal structure, Lengenbach, Binn Valley, Switzerland.

Introduction

Among the world-class localities for the study of sulfosalt assemblages, Lengenbach occupies an outstanding position, owing to the large number of sulfosalt species (more than 30 species as of November 2014) having there their type locality and to the complex and intriguing geochemistry, with the original combination of numerous cations (Pb, Tl, Ag, Cu, Zn, Cd, Sn, As, and Sb). In particular, Lengenbach can be considered the most important locality world-wide for the study of the crystal-chemistry of thallium sulfosalts. Indeed, 18 thallium sulfosalts have been identified from the Lengenbach dolostone so far; among these, fourteen were first described from this locality (Table 1).

Following the sulfosalt systematics given by Moëlo *et al*. (2008), thallium sulfosalts from Lengenbach can be classified in the following groups (the very recently approved mineral spaltiite is not considered because its crystallographic data have not been published yet):

i) sulfosalts with atom ratio of cation/chalcogen = 1: the hatchite isotypes (hatchite, wallisite) and the two members of the weissbergite homeotypic pair, *i.e*. weissbergite and lorándite;

ii) lead sulfosalts based on large 2D fragments of PbS/SnS archetype, represented by members of the sartorite homologous series (philrothite) and related compounds (dalnegroite, parapierrotite);

iii) specific Tl sulfosalts (structures with SnS layers), particularly represented by members of the hutchinsonite merotypic series (bernardite, hutchinsonite, edenharterite, jentschite, imhofite). Other minerals belonging to this type are sicherite, gabrielite, and ernigglite. Possibly, the recently described mineral raberite could be classified within this group;

iv) sulfosalts with an excess of small monovalent cations (Ag,Cu) relatively to (As, Sb, Bi), represented by the member of the routhierite isotypic series stalderite.

This latter mineral, as well as the members of the routhierite isotypic series, deserves a careful study, owing to their variable crystal chemistry, possibly reflecting the geochemistry of the crystallizing medium, as described for the routhierite – arsiccioite pair by Biagioni *et al*. (2014b). Preliminary EDS chemical analyses performed on specimens of stalderite showed the occurrence of Ag- and Fe-rich varieties. In particular, a specimen examined in 2003 proved to be an Ag-rich Fe-bearing stalderite. In 2013, new EDS chemical analyses confirmed its high Ag content, suggesting the need of a more accurate characterization.

Crystallographic studies and chemical analyses allowed us to describe this phase as the new mineral ralphcannonite. The mineral and its name have been approved by the CNMNC-IMA (2014-077). The holotype specimen of ralphcannonite is deposited in the mineralogical collection of the Museo di Storia Naturale, Università degli Studi di Firenze, Via La Pira 4, Florence, Italy, under catalog number 3145/I. The name honours Ralph Cannon (b. 1956) for his contribution to the knowledge of the mineralogy of the Lengenbach quarry. Ralph Cannon started working in the Lengenbach quarry in 1996. In 2003, when the Lengenbach Research Association (FGL, *Forschungsgemeinschaft Lengenbach*) was founded, he was appointed as Technical Head for specimen extraction, an activity he has been carrying out since with great dedication and intuition. He has also analyzed several specimens from this locality and has published many papers about Lengenbach mineralogy.

The aim of this paper is the description of the new mineral species ralphcannonite and its relationships with the other members of the routhierite isotypic series.

Occurrence and mineral description

The Lengenbach quarry (latitude 46°21'54''N, longitude 8°13'15''E) exploits a Triassic dolostone overlying the gneiss basement at the northern front of the Monte Leone Nappe, in the Penninic Domain of the Alps. These rocks have been metamorphosed up to upper greenschist – lower amphibolites facies conditions. The dolostone are 240 m thick at Lengenbach; mineralization occurs in the uppermost part of the sequence, close to the contact with the overlying Jurassic to Lower Cretaceous *Bündnerschiefer*. Hofmann and Knill (1996) recognized four major types of mineralization: *i*) stratiform layers of pyrite with minor galena, sphalerite, and xenomorphic sulfosalts; *ii*) massive to interstitial sulfosalt accumulations; *iii*) discordant sulfosalt and sulfide veins; and *iv*) idiomorphic crystals within druses and open fissures. Ralphcannonite was discovered in the type *ii*) mineralization, corresponding to the so-called "Zone 1" of Graeser *et al*. (2008). The studied specimen was originally found in 1989 by the *Arbeitsgemeinschaft Lengenbach* (Lengenbach Working Association). Via the Natural History Museum in Berne, the specimen found its way to the private collection of one of the authors (TR).

Physical and optical properties

Ralphcannonite was observed as euhedral crystals; on the basis of SEM images (Fig. 1) and the crystal forms reported by Graeser *et al*. (1995) for stalderite, the dominant forms could be the prism {110} and the basal pynacoid {001}, with the bipyramids {101} and {111}, as well as the prism {100} as accessory forms. Ralphcannonite is brittle, with irregular fracture; streak is black, luster is metallic. Micro-indentation measurements carried out with a VHN load of 30 g give a mean value of 120 kg·mm^{-2} (range: 116–128; 3 measurements) corresponding to a Mohs hardness of about 2–2½.

In plane-polarized incident light, ralphcannonite is greyish in color. Under crossed polars, it is very weakly anisotropic, with greyish to light blue rotation tints. Internal reflections are very weak. There is no optical evidence of growth zonation.

Reflectance measurements were performed in air by means of a MPM-200 Zeiss microphotometer equipped with a MSP-20 system processor on a Zeiss Axioplan ore microscope. The filament temperature was approximately 3350 K. An interference filter was adjusted, in turn, to select four wavelengths (approximating those recommended by the Commission on Ore Mineralogy of the IMA) for measurement (471.1, 548.3, 586.6, and 652.3 nm). Readings were taken for specimen and standard (SiC) maintained under the same focus conditions. The diameter of the circular measuring area was 0.1 mm. Reflectance percentages for R_{min} and R_{max} are 25.8, 27.1 (471.1 nm), 25.2, 26.6 (548.3 nm), 24.6, 25.8 (586.6 nm), and 23.9, 24.8 (652.3 nm), respectively.

Owing to the small amount of available pure material, the density was not measured; the calculated density, based on the empirical formula (see below), is 4.927 g·cm^{-3}.

In the studied specimen, ralphcannonite is associated with hatchite, dufrénoysite, realgar, and baryte.

Chemical analysis

A preliminary chemical analysis using EDS performed on the crystal fragment used for the single-crystal X-ray diffraction did not indicate the presence of elements ($Z > 9$) other than Fe, Cu, Zn, As, Ag, Hg, Tl, and S.

The same fragment was then analyzed with a JEOL 8200 electron microprobe (WDS mode, accelerating voltage 15 kV, beam current 20 nA, beam size 1 μm). Counting times are 20 s for peak and 15 s for background. The following standards (element, emission line) were used: Ag metal (Ag *L*α), Cu metal (Cu *K*α), Zn metal (Zn *K*α), Fe metal (Fe *K*α), cinnabar (Hg *M*α), $TlAsS_2$ (Tl *M*α, S *K*α), As metal (As *L*α), and Sb metal (Sb *L*α). Cadmium and Se were sought but found below the detection limit. The crystal fragment was found to be homogeneous within analytical error. Chemical data are given in Table 2.

On the basis of 12 atoms per formula unit (*apfu*), the chemical formula of ralphcannonite corresponds to $Ag_{0.63(2)}Cu_{0.25(2)}Zn_{1.35(5)}Fe_{0.47(1)}Hg_{0.32(2)}Tl_{0.97(3)}[As_{1.97(6)}Sb_{0.01(1)}]_{\Sigma 1.98(5)}S_{6.03(8)}$.

Crystallography

For the X-ray single-crystal studies, the intensity data were collected using an Oxford Diffraction Xcalibur 3 diffractometer equipped with a Sapphire 2 CCD area detector, with Mo *K*α radiation. The detector to crystal distance was 60 mm. 288 frames were collected using ω scan mode, in 0.5° slices, with an exposure time of 45 seconds per frame. Intensity integration and standard Lorentz-polarization corrections were performed with the *CrysAlis* RED (Oxford Diffraction, 2006) software package. The program ABSPACK in *CrystAlis* RED (Oxford Diffraction, 2006) was used for the absorption correction. The statistical tests on the distribution of $|E|$ values ($|E^2-1| = 0.808$) and the systematic absences suggested the space group $I\bar{4}2m$. The refined cell parameters are a 9.861(2), c 11.125(3) Å, V 1081.8(4) Å^3

The crystal structure of ralphcannonite was refined starting from the atomic coordinates given by Bindi (2008) for routhierite, using Shelxl-97 (Sheldrick, 2008). Scattering curves for neutral atoms were taken from the *International Tables for Crystallography* (Wilson, 1992). Crystal data and details of intensity data collection and refinement are reported in Table 3. Owing to the relatively low number of observed reflections, only an isotropic model was refined for ralphcannonite. After several cycles of refinement, the R_1 converged to 0.030, confirming the validity of the structural model. Four independent cation sites occur in the crystal structure of ralphcannonite, labelled as Tl, *M*1, *M*2, and As. *M*1 and *M*2 sites correspond to Cu and Hg sites in the crystal structure of routhierite (Bindi, 2008; Biagioni *et al*., 2013). The occupancies of these four independent cation sites were refined using the following scattering curves: Tl site: Tl vs □; *M*1 site: Cu vs □; *M*2 site: Hg vs □; As site: As vs □. Tl, *M*1, and As sites were found to be fully occupied and their site occupancies were fixed to 1. At the *M*2 site, the refined site scattering value was 43.9 electrons, compatible with a mixed (Ag,Zn,Fe,Hg) occupancy. Final atom coordinates and isotropic displacement parameters are given in Table 4, whereas selected bond distances are reported in Table 5. Table 6 gives the refined and calculated site scattering (in electrons per formula unit, *epfu*) on the basis of the proposed site populations. Fe has been considered

as divalent, in order to achieve the electrostatic neutrality; this is consistent with the observation of Makovicky *et al*. (1990) that the presence of Zn and Hg favours Fe^{2+} with respect to Fe^{3+}. Finally, Table 7 shows the results of the bond valence calculations.

Owing to the very small size and the low amount of the available crystals, X-ray powder diffraction pattern was not collected. Table 8 reports the calculated X-ray powder diffraction data of ralphcannonite on the basis of the crystallographic data collected through single-crystal X-ray diffraction.

Crystal structure description

The crystal structure of ralphcannonite is isotypic with those of routhierite, stalderite, and arsiccioite (Graeser *et al*., 1995; Bindi, 2008; Biagioni *et al*., 2014a; Biagioni *et al*., 2014b), showing a framework formed by two independent MeS_4 tetrahedra sharing corners, hosting channels parallel to [001]. These channels contain TlS_6 and $(As,Sb)S_3$ polyhedra, sharing corners and edges with the tetrahedron framework (Fig. 2).

As stated above, four independent cation sites occur. The two independent tetrahedral sites, *M*1 and *M*2, have average bond distances of 2.358 and 2.468 Å, respectively. The <*M*1–S> bond distance closely agrees with that observed by Graeser *et al*. (1995) for the Cu site of stalderite, *i.e*. 2.357(4) Å, whereas the *M*2 site of ralphcannonite is enlarged with respect to the corresponding Zn site of stalderite, having an average bond distance of 2.406 Å. This is in agreement with the replacement of the small Zn (and possibly Cu) atoms by the larger Ag at the *M*2 site.

The As site forms a trigonal pyramid with three S atoms, with an average bond distance of 2.257 Å. The refinement of the site occupancy points to the full occupancy of this site by arsenic, in agreement with chemical data showing only negligible amount of Sb (0.01 *apfu*). Actually the AsS_3 geometry is distorted, with two relatively short As–S1 bond distance (2.198 Å) and a longer one (2.378 Å).

The coordination of the Tl site can be described as an orthorhombic pyramid with a split apex, as in the other members of the routhierite isotypic series. On the other site of the pyramidal split apex, a relatively short Tl–Tl distance occur, i.e. 3.284(4) Å. This value perfectly agrees with that reported for stalderite (3.28 Å) by Graeser *et al*. (1995) and is in the range of Tl–Tl distances observed in other members of the routhierite group, i.e. 3.33 Å and 3.47 Å for routhierite from Monte Arsiccio and Jas Roux, respectively (Bindi, 2008; Biagioni *et al*., 2014a) and values ranging between 3.25 and 3.51 Å for the split Tl site in arsiccioite (Biagioni *et al*., 2014b). As reported by previous authors, such short Tl–Tl distances most likely indicate some type of Tl–Tl interaction.

Bond-valence balance

Bond valence sums (BVS), according to Brese and O'Keeffe (1991), are reported in Table 7, on the basis of the site population given in Table 6.

With respect to the BVSs of routhierite and arsiccioite, where differences up to 25% between observed and calculated BVS have been reported (Biagioni *et al*., 2014a; Biagioni *et al*., 2014b), only minor deviations from the expected values (up to 7% for the *M*2 site) have been observed, confirming the validity of the proposed site population. A good agreement

between observed and calculated BVS occurs also for the As site. The BVS excess for the Tl atom is similar to that reported in arsiccioite and routhierite (Biagioni *et al*., 2014a; Biagioni *et al*., 2014b) and can be related to the overestimation of the bond parameter tabulated by Brese and O'Keeffe (1991) for the pair (Tl,S), *i.e*. 2.63 Å, as suggested by Biagioni *et al*. (2014b). Using a value of $R_{Tl,S}$ = 2.55 Å, a BVS of 0.95 valence units (*v.u*.) can be calculated for the Tl site.

Crystal chemistry

Structural formula

The crystal-chemical formula of ralphcannonite can be written as $^{M1}(Zn_{0.75}Cu_{0.25})^{M2}(Ag_{0.32}Zn_{0.29}Fe_{0.23}Hg_{0.16})_2TlAs_2S_6$, with the relative error of the valence equilibrium Ev = + 0.9.

Graeser *et al*. (1995) proposed that in stalderite the small *M*1 site is occupied by Cu^+, whereas the divalent cations (Zn^{2+} and minor Fe^{2+} and Hg^{2+}) are hosted at the larger *M*2 site. On the contrary, the results of the crystal structure study suggest that *M*1 is preferentially occupied by Zn^{2+}, whereas *M*2 hosts the larger cations Ag^+ and Hg^{2+}, replaced by Zn^{2+} and Fe^{2+}. As reported by Biagioni *et al*. (2014b) for arsiccioite, the cation distribution among the *M*1 and *M*2 sites is guided by the steric constraint that prevails over the valence state. Therefore, the largest cation, Ag^+ is hosted at the large *M*2 site, whereas Zn^{2+}, the smallest cation, preferentially occupies the M1 site.

Similarly to the ideal formula of arsiccioite, $^{M1}Hg^{M2}(Ag_{0.5}Hg_{0.5})_2TlAs_2S_6$, the formula of ralphcannonite could be written $^{M1}Zn^{M2}(Ag_{0.5}Zn_{0.5})_2TlAs_2S_6$. The Ag content of ralphcannonite is actually a little lower than the ideal one, and its deficit is probably balanced through the heterovalent substitution $^{M1}Zn^{2+} + {}^{M2}Ag^+ \rightarrow {}^{M1}Cu^+ + {}^{M2}(Zn,Fe,Hg)^{2+}$.

Nomenclature of the routhierite isotypic series

The general crystal-chemical formula of the members of the routhierite isotypic series can be written as $(Me^+_{1-2x}Me^{2+}_{2x})(Me^{2+}_{1-x}Me^+_x)_2Tl(As_{1-y}Sb_y)_2S_6$, with $0 \leq x \leq 0.5$, and $y < 0.5$. Me^+ is represented by Cu^+ and Ag^+, whereas bivalent cations Me^{2+} are Zn^{2+}, Hg^{2+}, and Fe^{2+}. Minor Cd^{2+} (up to 0.02 *apfu*) has been reported in arsiccioite (Biagioni *et al*., 2014b).

The crystal structure studies of arsiccioite and ralphcannonite indicate that Ag prefers the largest *M*2 site; this observation can be extended also to Ag-bearing routhierite (*e.g*., specimen from Monte Arsiccio – Biagioni *et al*., 2014a; Biagioni *et al*., 2014b). On the contrary, the smaller cations (Zn^{2+}, Cu^+) are preferentially hosted at the *M*1 site.

Graeser *et al*. (1995), in their study of stalderite, proposed the site population *M*1 = $Cu_{1.00}$ and *M*2 = $Zn_{0.55}Fe_{0.25}Hg_{0.20}$; however, as pointed out by Biagioni *et al*. (2014b), a site population with *M*1 = $Zn_{1.00}$, and *M*2 = $Cu_{0.50}Fe_{0.25}Hg_{0.20}Zn_{0.05}$ cannot be excluded, resulting in very similar site scattering values, BVS, and calculated average bond distances. Consequently, one could verify a different cation distribution also for ralphcannonite, with Zn completely hosted at the *M*1 site and a mixed (Ag,Cu,Fe,Hg,Zn) occupancy at the *M*2 site. In this case, the idealized site population should be *M*1 = $Zn_{1.00}$ and *M*2 = $Ag_{0.32}Cu_{0.13}Fe_{0.23}Hg_{0.16}Zn_{0.16}$. Assuming such a distribution, the BVSs, average bond distances, and calculated site scattering are similar to those proposed in Table 6, suggesting

that the actual site occupancy, by using conventional X-ray diffraction, cannot be known, owing to the similar values of the scattering factors for Cu, Zn, and also Fe. It is noteworthy that the site population proposed in Table 6 would correspond to the ideal formula $Zn(Ag_{0.5}Zn_{0.5})_2TlAs_2S_6$, whereas in the alternative cation distribution such formula should be written as $Zn(Ag_{0.5}Fe_{0.5})_2TlAs_2S_6$, being Fe^{2+} the dominant bivalent cation at *M*2. Consequently, the same chemistry could correspond to two different crystal chemical formulae. Taking into account this issue, in our opinion, the classification of the members of the routhierite isotypic series should be based on the chemical data only, taking into account the combination of dominant Me^+ and Me^{2+} cations. In this way the following species can be defined (Fig. 3):

i) routhierite – $Me^+ = Cu^+$, $Me^{2+} = Hg^{2+}$;
ii) stalderite – $Me^+ = Cu^+$, $Me^{2+} = Zn^{2+}$;
iii) arsiccioite – $Me^+ = Ag^+$, $Me^{2+} = Hg^{2+}$;
iv) ralphcannonite – $Me^+ = Ag^+$, $Me^{2+} = Zn^{2+}$,
being the general chemical formula $Me^+Me^{2+}_2TlAs_2S_6$.

Relationships between the crystal-chemistry of "routhierites" and the ore geochemistry

The members of the routhierite isotypic series are very rare minerals. Well-characterized specimens of routhierite have been reported so far only from Jas Roux, France, and the Monte Arsiccio mine, Italy (Johan *et al*., 1974; Biagioni *et al*., 2014a). The other three phases have been reported only from their type-locality, Monte Arsiccio mine (arsiccioite – Biagioni *et al*., 2014b), and the Lengenbach quarry (stalderite – Graeser *et al*., 1995; ralphcannonite – this work).

These minerals can have a complex chemistry, being characterized by the occurrence of Tl, As, Cu, Ag, Hg, Zn, and minor Fe and Sb. In particular, the chemical variability of the tetrahedral cations (Cu, Ag, Hg, Zn, and Fe) seems to be closely related to the ore geochemistry, as discussed by Biagioni *et al*. (2014b) for the pair routhierite-arsiccioite from Monte Arsiccio. This locality, as well as Jas Roux, are characterized by a relatively abundance of Hg, as evidenced by the occurrence of the Hg members of the routhierite isotypic series, as well as other Hg phases, *i.e*. aktashite, $Cu_6Hg_3As_4S_{12}$, and laffittite, $AgHgAsS_3$ (Favreau *et al*., 2011; Biagioni *et al*., 2014c).

The ore geochemistry at the Lengenbach quarry, on the contrary, seems to be Hg-depleted. In fact, the Zn-dominant (sometimes Fe-enriched) members of the routhierite isotypic series occur there, stalderite and ralphcannonite. In addition, the Zn isotype of aktashite, nowackiite, $Cu_6Zn_3As_4S_{12}$, has been identified (Marumo and Burri, 1965). The variable Ag/Cu ratio within the crystallizing medium controls the crystallization of the stalderite – ralphcannonite pair, as well as other isotypic compounds described from the Lengenbach quarry, e.g. hatchite, $AgTlPbAs_2S_5$, and wallisite, $CuTlPbAs_2S_5$

Conclusion

The description of ralphcannonite increases the knowledge about the crystal chemistry of the routhierite isotypic series, bringing new data to the systematics of thallium sulfosalts. The unexpected cation distribution described by Biagioni *et al*. (2014b) in arsiccioite has been confirmed, with Ag, the largest cation, preferentially hosted at the largest *M*2 site: the priority

of the steric effect over the valence state in the members of the routhierite isotypic series is thus confirmed.

Acknowledgements

The research was supported by “progetto d’Ateneo 2012. Università di Firenze” to LB.

REFERENCES

Biagioni, C., Bonaccorsi, E., Moëlo, Y. and Orlandi, P. (2014a) Mercury-arsenic sulfosalts from Apuan Alps (Tuscany, Italy). I. Routhierite, $(Cu_{0.8}Ag_{0.2})Hg_2Tl(As_{1.4}Sb_{0.6})_{\Sigma=2}S_6$, from Monte Arsiccio mine: occurrence and crystal structure. *European Journal of Mineralogy*, **26**, 163–170.

Biagioni, C., Bonaccorsi, E., Moëlo, Y., Orlandi, P., Bindi, L., D'Orazio, M. and Vezzoni, S. (2014b) Mercury-arsenic sulfosalts from the Apuan Alps (Tuscany, Italy). II. Arsiccioite, $AgHg_2TlAs_2S_6$, a new mineral from the Monte Arsiccio mine: occurrence, crystal structure and crystal chemistry of the routhierite isotypic series. *Mineralogical Magazine*, **78**, 101–117.

Biagioni, C., Bonaccorsi, E., Moëlo, Y. and Orlandi, P. (2014c) Mercury-arsenic sulfosalts from the Apuan Alps (Tuscany, Italy). III. Aktashite, $Cu_6Hg_3As_4S_{12}$, and laffittite, $AgHgAsS_3$ from the Monte Arsiccio mine: occurrence and crystal structure. *Periodico di Mineralogia*, **83**, 1–18.

Bindi, L. (2008) Routhierite, $Tl(Cu,Ag)(Hg,Zn)_2(As,Sb)_2S_6$. *Acta Crystallographica*, **C64**, i95–i96.

Bindi, L., Nestola, F., Guastoni, A., Peruzzo, L., Ecker, M. and Carampin, R. (2012b) Raberite, $Tl_5Ag_4As_6SbS_{15}$, a new Tl-bearing sulfosalt from Lengenbach quarry, Binn Valley, Switzerland: description and crystal structure. *Mineralogical Magazine*, **76**, 1153–1163.

Bindi, L., Nestola, F., Makovicky, E., Guastoni, A. and Debattisti, L. (2014) Tl-bearing sulfosalt from Lengenbach quarry, Binn Valley, Switzerland: Philrothite, $TlAs_3S_5$. *Mineralogical Magazine*, **78**, 1–9.

Brese, N.E. and O'Keeffe, M. (1991) Bond-valence parameters for solids. *Acta Crystallographica*, **B47**, 192–197.

Burri, G., Graeser, S., Marumo, F. and Nowacki, W. (1965) Imhofit, ein neues thallium-arsensulfosalz aus dem Lengenbach (Binnatal, Kanton Wallis). *Chimia*, **19**, 499–500.

Favreau, G., Bourgoin, V. and Bouillard, J.C. (2011) Jas Roux: un gisement exceptionel à minéraux de thallium. *Le Cahier des Micromonteurs*, **113**, 2–91.

Graeser, S. (1967) Ein Vorkommen von Lorandit ($TlAsS_2$) der Schweiz. *Contributions to Mineralogy and Petrology*, **16**, 45–50.

Graeser, S. and Edenharter, A. (1997) Jentschite ($TlPbAs_2SbS_6$) – a new sulphosalt mineral from Lengenbach, Binntal (Switzerland). *Mineralogical Magazine*, **61**, 131–137.

Graeser, S. and Schwander, H. (1992) Edenharterite ($TlPbAs_3S_6$): a new mineral from Lengenbach, Binntal (Switzerland). *European Journal of Mineralogy*, **4**, 1265–1270.

Graeser, S., Schwander, H., Wulf, R. and Edenharter, A. (1992) Ernigglite ($Tl_2SnAs_2S_6$), a new mineral from Lengenbach, Binntal (Switzerland): description and crystal structure determination based on data from synchrotron radiation. *Schweizerische Mineralogische und Petrographische Mitteilungen*, **72**, 293–305.

Graeser, S., Schwander, H., Wulf, R. and Edenharter, A. (1995) Stalderite, $TlCu(Zn,Fe,Hg)_2As_2S_6$ – a new mineral related to routhierite: description and crystal structure. *Schweizerische Mineralogische und Petrographische Mitteilungen*, **75**, 337–345.

Graeser, S., Berlepsch, P., Makovicky, E. and Balić-Žunić, T. (2001) Sicherite, $TlAg_2(As,Sb)_3S_6$, a new sulfosalt mineral from Lengenbach (Binntal, Switzerland): description and structure determination. *American Mineralogist*, **86**, 1087–1093.

Graeser, S., Topa, D., BaliC-Žunić, T. and Makovicky, E. (2007) Gabrielite, $Tl_2AgCu_2As_3S_7$, a new species of thallium sulfosalt from Lengenbach, Binntal, Switzerland. *The Canadian Mineralogist*, **44**, 135–140.

Graeser, S., Cannon, R., Drechsler, E., Raber, T., and Roth, P. (2008) Faszination Lengenbach Abbau-Forschung-Mineralien 1958-2008. Kristallographik Verlag, Achberg, Germany, 192 p.

Graeser, S., Topa, D., Effenberger, H., Makovicky, E. and Paar, W.H. (2014) Spaltiite, IMA 2014-012. CNMNC Newsletter No. 20, June 2014, page 557. *Mineralogical Magazine*, **78**, 549–558.

Harris, D.C. (1989) The mineralogy and geochemistry of the Hemlo gold deposit, Ontario. *Geological Survey of Canada, Economic Geology Reports*, **38**, 88 pp.

Hofmann, B.A. and Knill, M.D. (1996) Geochemistry and genesis of the Lengenbach Pb-Zn-As-Tl-Ba mineralization, Binn Valley, Switzerland. *Mineralium Deposita*, **31**, 319–339.

Hofmann, B.A., Graeser, S., Imhof, T., Sicher, V. and Stalder, H.A. (1993) Mineralogie der Grube Lengenbach, Binntal, Wallis. Zum 35-jährigen Bestehen der Arbeitsgemeinschaft Lengenbach. *Jahrbuch Naturhistorische Museum Bern*, **1990-1992**, 3–90.

Johan, Z., Mantienne, J. and Picot, P. (1974) La routhiérite, $TlHgAsS_3$, et la laffittite, $AgHgAsS_3$, deux nouvelles espèces minerales. *Bulletin de la Société française de Minéralogie et de Cristallographie*, **97**, 48–53.

Kraus, W. and Nolze, G. (1996) PowderCell – a program for the representation and manipulation of crystal structures and calculation of the resulting X-ray powder patterns. *Journal of Applied Crystallography*, **29**, 301–303.

Makovicky, E., Forcher, K., Lottermoser, W. and Amthauer, G. (1990) The role of Fe^{2+} and Fe^{3+} in synthetic Fe-substituted tetrahedrite. *Mineralogy and Petrology*, **43**, 73–81.

Marumo, F. and Burri, G. (1965) Nowackiite, a new copper zinc arsenosulfosalt from Lengenbach (Binnatal, Kanton Wallis). *Chimia*, **19**, 500–501.

Moëlo, Y., Makovicky, E., Mozgova, N.N., Jambor, J.L., Cook, N., Pring., A., Paar, W.H., Nickel, E.H., Graeser, S., Karup-Møller, S., Balić-Žunić, T., Mumme, W.G., Vurro, F., Topa, D., Bindi, L., Bente, K. and Shimizu, M. (2008) Sulfosalt systematics: a review. Report of the sulfosalt sub-committee of the IMA Commission on Ore Mineralogy. *European Journal of Mineralogy*, **20**, 7–46.

Nestola, F., Guastoni, A., Bindi, L. and Secco, L. (2009) Dalnegroite, $Tl_{5-x}Pb_{2x}(As,Sb)_{21-x}S_{34}$, a new thallium sulphosalt from Lengenbach quarry, Binntal, Switzerland. *Mineralogical Magazine*, **73**, 1027–1032.

Nowacki, W. (1965) Über einige Mineralfunde aus dem Lengenbach (Binnatal, Kt. Wallis). *Eclogae Geologicae Helveticae*, **58**, 403–406.

Oxford Diffraction (2006) *CrysAlis* RED (Version 1.171.31.2) and ABSPACK in *CrysAlis* RED. Oxford Diffraction Ltd, Abingdon.

Roth, P., Raber, T., Drechsler, E. and Cannon, R. (2014) The Lengenbach Quarry, Binn Valley, Switzerland. *The Mineralogical Record*, **45**, 157–196.

Sheldrick, G.M. (2008) A short history of SHELX. *Acta Crystallographica*, **A64**, 112–122.

Solly, R.H. (1905) Some new minerals from the Binnenthal, Switzerland. *Mineralogical Magazine*, **14**, 72–82.

Solly, R.H. and Smith, G.F.H. (1912) Hatchite, a new (anorthic) mineral from the Binnenthal. *Mineralogical Magazine*, **16**, 287–289.

Wilson, A.J.C. (1992) International Tables for X-ray Crystallography Volume C. Kluwer, Dordrecht.

Table captions

Table 1. Thallium sulfosalts from Lengenbach. In bold, sulfosalts having their type-locality at Lengenbach.

Table 2. Microprobe analyses of ralphcannonite: chemical composition as wt% and number of atoms on the basis of 12 atoms per formula unit. Valence equilibrium: Ev (%) = [Σ(val+) – Σ(val–)]× 100/Σ(val–).

Table 3. Crystal and experimental data for ralphcannonite.

Table 4. Atomic coordinates and isotropic displacement parameters ($Å^2$) for ralphcannonite.

Table 5. Selected bond distances (in Å) in ralphcannonite.

Table 6. Refined site scattering values (*epfu*), assigned site population (*apfu*) and comparison between observed and calculated bond distances (in Å) at *M*1, *M*2, and As sites in ralphcannonite.

Table 7. Bond valence sums (BVS, in valence units, *vu*) calculated using the parameters given by Brese and O'Keeffe (1991).

Table 8. Calculated X-ray powder diffraction data for ralphcannonite. Intensity and d_{hkl} were calculated using the software Powdercell 2.3 (Kraus and Nolze, 1996) on the basis of the structural model given in Table 4; only reflections with $I_{calc} > 5$ are listed. The five strongest reflections are given in bold.

Figure captions

Fig. 1. Ralphcannonite, equant crystals on realgar.

Fig. 2. Crystal structure of ralphcannonite, as seen down [001] (a) and [010] (b). Polyhedra: green: *M*1 tetrahedra; light blue: *M*2 tetrahedra. Circles: grey: Tl site; violet: As site; yellow: S1 site; orange: S2 site.

Fig. 3. Ag/(Ag+Cu) versus Hg/(Hg+Zn+Fe) atomic ratios in the routhierite isotypic series. Open triangles: arsiccioite from Monte Arsiccio mine (Biagioni *et al*., 2014b). Filled triangles: routhierite from Monte Arsiccio mine (black, Biagioni *et al*., 2014b; grey, Biagioni *et al*., 2014a). Open circles: routhierite from Jas Roux (Johan *et al*., 1974). Filled circles: routhierite from Jas Roux (Bindi, 2008). Open squares: stalderite from Lengenbach (Graeser *et al*., 1995). Filled squares (red): ralphcannonite (this work). Filled lozenges: "Sb-routhierite" from Hemlo (Harris, 1989).

Table 1. Thallium sulfosalts from Lengenbach. In bold, sulfosalts having their type-locality at Lengenbach.

Mineral	Chemical formula	References
Bernardite	$TlAs_5S_8$	Hofmann *et al*. (1993)
Dalnegroite	$(Tl_2PbSb)(Sb_3As_6)S_{17}$	Nestola *et al*. (2009)
Edenharterite	$TlPbAs_3S_6$	Graeser and Schwander (1992)
Ernigglite	$SnTl_2As_2S_6$	Graeser *et al*. (1992)
Gabrielite	$Cu_2AgTl_2As_3S_7$	Graeser *et al*. (2007)
Hatchite	$AgTlPbAs_2S_5$	Solly and Smith (1912)
Hutchinsonite	$TlPbAs_5S_9$	Solly (1905)
Imhofite	$Tl_{5.8}As_{15.4}S_{26}$	Burri *et al*. (1965)
Jentschite	$TlPbAs_2SbS_6$	Graeser and Edenharter (1997)
Lorándite	$TlAsS_2$	Graeser (1967)
Parapierrotite	$TlSb_5S_8$	Nestola (unp. data, 2014)
Philrothite	$TlAs_3S_5$	Bindi *et al*. (2014)
Raberite	$Ag_4Tl_5As_6SbS_{15}$	Bindi *et al*. (2012b)
Ralphcannonite	$AgZn_2TlAs_2S_6$	this work
Sicherite	$Ag_2Tl(As,Sb)_3S_6$	Graeser *et al*. (2001)
Spaltiite	$Cu_2Tl_2As_2S_5$	Graeser *et al*. (2014)
Stalderite	$CuZn_2TlAs_2S_6$	Graeser *et al*. (1995)
Wallisite	$CuTlPbAs_2S_5$	Nowacki (1965)
Weissbergite	$TlSbS_2$	Roth *et al*. (2014)

Table 2. Microprobe analyses of ralphcannonite: chemical composition as wt% and number of atoms on the basis of 12 atoms per formula unit. Valence equilibrium: Ev (%) = [Σ(val+) – Σ(val–)]× 100/Σ(val–).

Element	wt%	range	e.s.d.
Cu	2.01	1.78 – 2.22	0.06
Ag	8.50	8.19 – 8.80	0.16
Zn	10.94	10.25 – 11.33	0.20
Fe	3.25	3.10 – 3.34	0.08
Hg	7.92	7.10 – 8.50	0.12
Tl	24.58	23.87 – 25.26	0.26
As	18.36	17.58 – 18.96	0.19
Sb	0.17	0.09 – 0.25	0.04
S	24.03	23.61 – 24.66	0.21
Total	99.76	99.25 – 100.88	0.71

	apfu	range	e.s.d.
Cu	0.255	0.226 – 0.279	0.022
Ag	0.634	0.606 – 0.663	0.021
Zn	1.346	1.262 – 1.400	0.054
Fe	0.468	0.449 – 0.482	0.013
Hg	0.318	0.286 – 0.344	0.022
Tl	0.968	0.940 – 1.005	0.028
As	1.972	1.908 – 2.037	0.057
Sb	0.011	0.006 – 0.016	0.004
S	6.030	5.949 – 6.141	0.78
Ev	0.1	–3.7 – 3.0	2.5

Table 3. Crystal and experimental data for ralphcannonite.

Crystal data	
Crystal size (mm^3)	0.0035 x 0.045 x 0.055
Cell setting, space group	Tetragonal, $I\bar{4}2m$
a, c (Å);	9.861(2), 11.125(3)
V ($Å^3$)	1081.8(4)
Z	4
Data collection and refinement	
Radiation, wavelength (Å)	Mo$K\alpha$, λ = 0.71073
Temperature (K)	293
$2\theta_{max}$	56.05
Measured reflections	7722
Unique reflections	633
Reflections with $F_o > 4\sigma(F_o)$	140
R_{int}	0.0408
$R\sigma$	0.0498
Range of h, k, l	$-7 \le h \le 8$, $0 \le k \le 12$, $0 \le l \le 13$
R [$F_o > 4\sigma(F_o)$]	0.0299
R (all data)	0.0420
wR (on F^2)	0.1048
Number of least-squares parameters	20
Maximum and minimum residual peak (e $Å^{-3}$)	0.93 (at 1.94 Å from S2) -1.86 (at 1.19 Å from Tl)

Table 4. Atomic coordinates and isotropic displacement parameters (Å^2) for ralphcannonite.

Site	Wyckoff site	*x*/*a*	*y*/*b*	*z*/*c*	U_{iso}
Tl	4*e*	0	0	0.3524(2)	0.0413(7)
*M*1	4*d*	0	½	¼	0.0334(14)
*M*2	8*f*	0.2228(2)	½	½	0.0405(11)
As	8*i*	0.2611(4)	0.2611(4)	0.2587(6)	0.0400(12)
S1	16*j*	0.0943(6)	0.3308(7)	0.3743(7)	0.037(2)
S2	8*i*	0.1257(7)	0.1257(7)	0.1295(9)	0.040(3)

Table 5. Selected bond distances (in Å) in ralphcannonite.

Tl	– S2	3.037(10) × 2	*M*1	– S1	2.358(7) × 4
	– S1	3.401(7) × 4			
	average	3.280			
As	– S1	2.198(8) × 2	*M*2	– S1	2.417(6) × 2
	– S2	2.374(11)		– S2	2.519(7) × 2
	average	2.257		average	2.468

Table 6. Refined site scattering values (*epfu*), assigned site population (*apfu*) and comparison between observed and calculated bond distances (in Å) at *M*1, *M*2, and As sites in ralphcannonite.

Site	XRD	EPMA	Site population	$\langle Me–S \rangle_{obs}$	$\langle Me–S \rangle_{calc}$
*M*1	29.0	29.8	$[Zn_{0.751}Cu_{0.249}]$*	2.358	2.352
*M*2	43.8	42.4	$Ag_{0.317}Zn_{0.290}Fe_{0.234}Hg_{0.159}$	2.468	2.499
As	33.0	33.1	$[As_{0.995}Sb_{0.005}]$*	2.257	2.261

*Values normalized to 1

Table 7. Bond valence sums (BVS, in valence units, *vu*) calculated using the parameters given by Brese and O'Keeffe (1991).

	*M*1	*M*2	Tl	As	Σ anions
S1	0.43^{x4}	0.51^{x2}	0.12^{x4}	1.17^{x2}	2.23
S2		$^{2x}0.39^{x2}$	0.34^{x2}	0.74	1.86
Σ cations	1.72	1.80	1.16	3.08	
Theor.	1.75	1.68	1.00	3.00	

In mixed sites, bond-valence contribution of each cation has been weighted according to its occupancy (see Table 5). Left and right superscripts indicates the number of bonds involving cations and anions, respectively.

Table 8. Calculated X-ray powder diffraction data for ralphcannonite. Intensity and d_{hkl} were calculated using the software Powdercell 2.3 (Kraus and Nolze, 1996) on the basis of the structural model given in Table 4; only reflections with $I_{calc} > 5$ are listed. The five strongest reflections are given in bold.

I_{calc}	d_{calc}	*h k l*	I_{calc}	d_{calc}	*h k l*
8	6.973	1 1 0	5	2.324	3 3 0
9	4.930	2 0 0	8	2.201	3 2 3
85	**4.100**	**2 1 1**	14	2.076	3 1 4
12	3.486	2 2 0	10	2.010	4 1 3
40	**3.471**	**1 0 3**	10	1.845	4 0 4
17	3.118	3 1 0	15	1.807	5 2 1
100	**2.954**	**2 2 2**	13	1.743	4 4 0
20	2.656	3 2 1	9	1.741	4 3 3
17	2.583	1 1 4	9	1.728	4 2 4
24	**2.465**	**4 0 0**	6	1.604	6 1 1
39	**2.460**	**3 0 3**	6	1.594	3 1 6
11	2.422	2 0 4	7	1.588	5 1 4
6	2.338	4 1 1	11	1.501	6 2 2

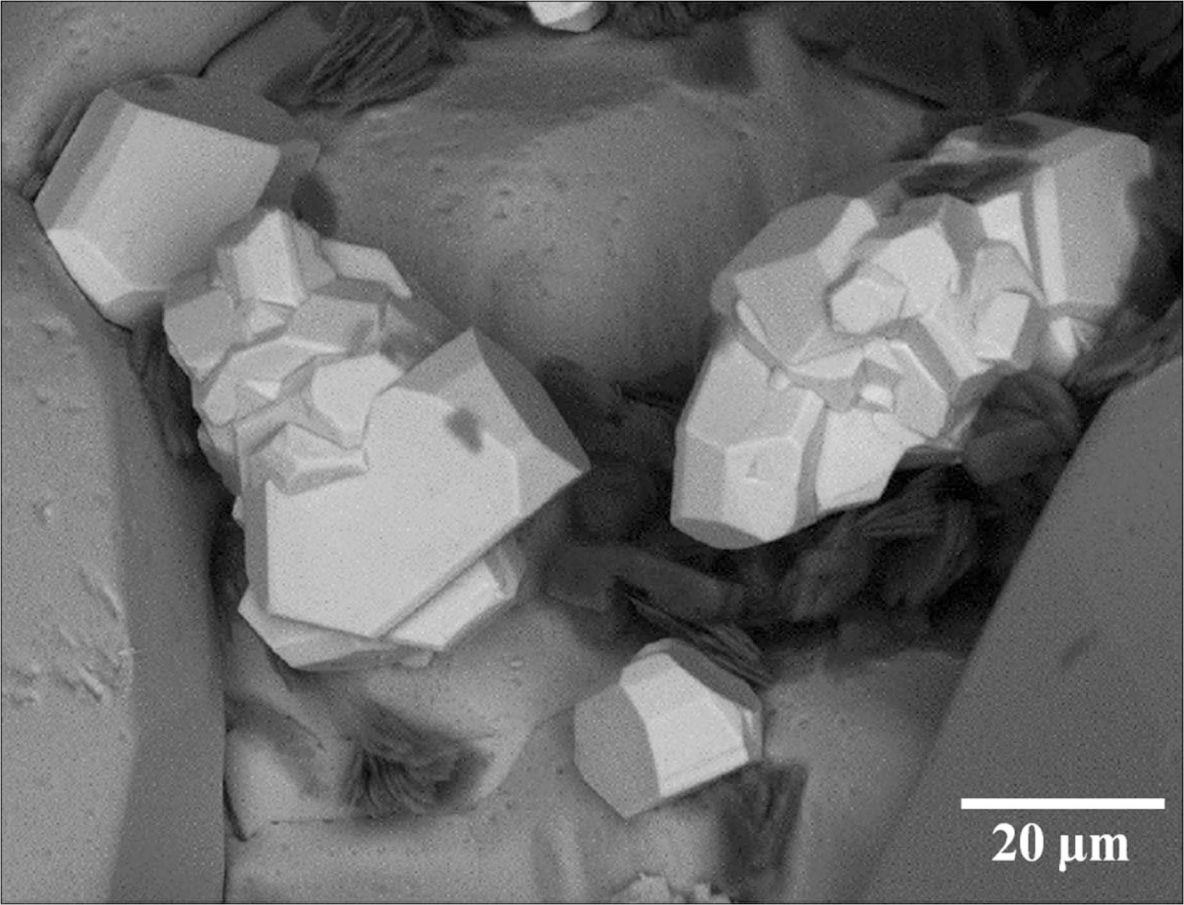
20 µm

(a)

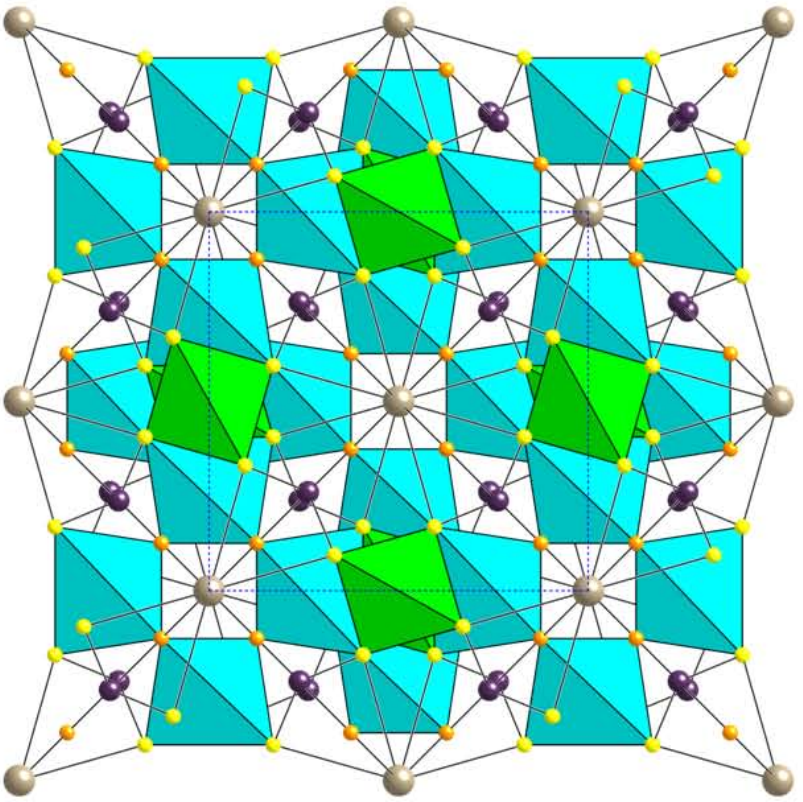

(b)

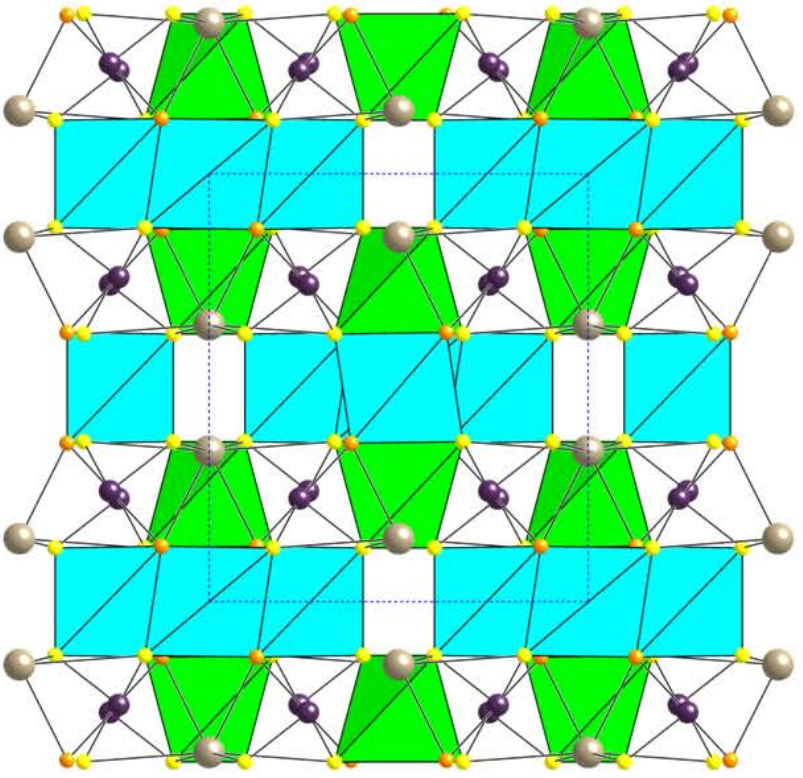

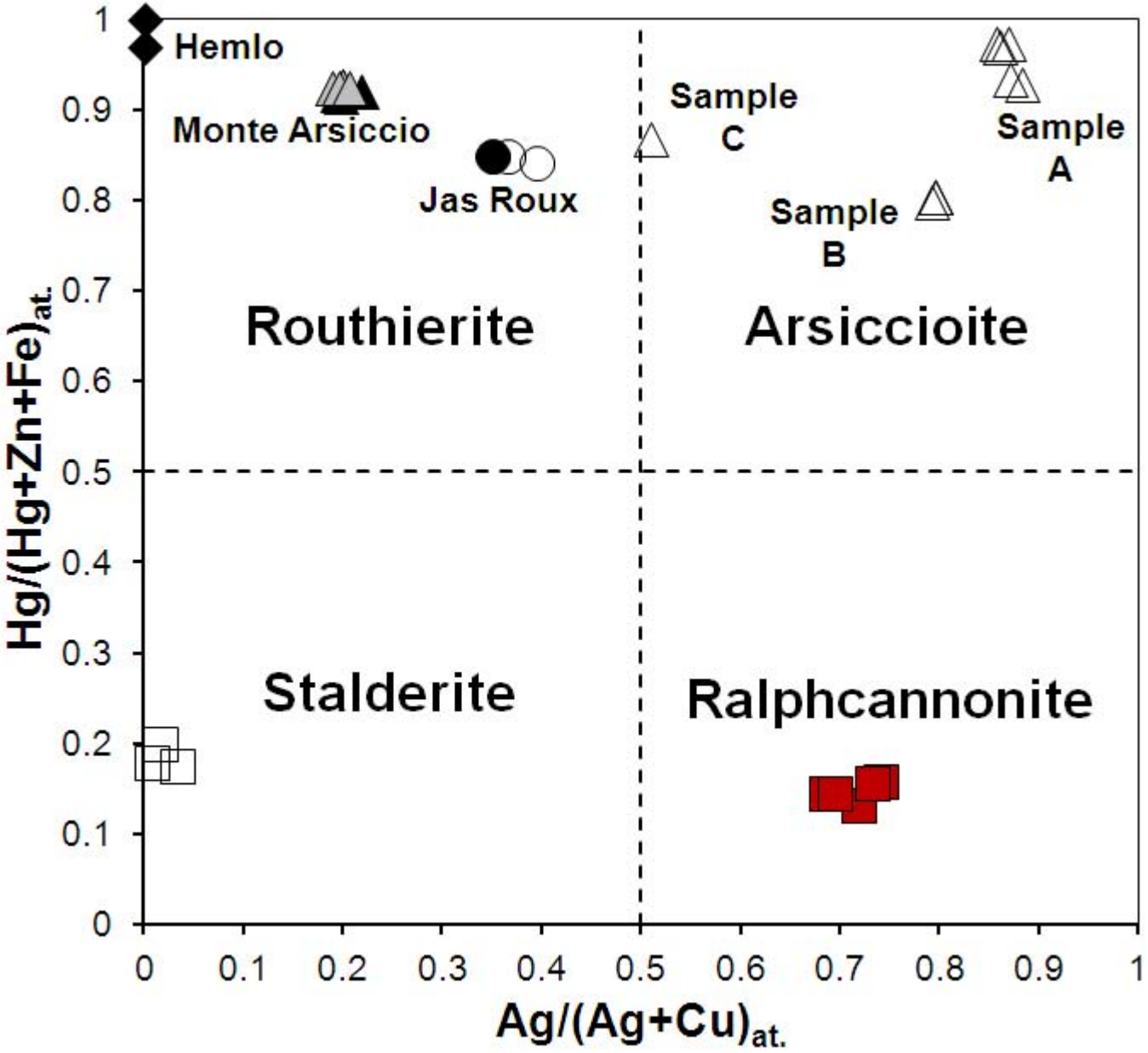
Hemlo
Monte Arsiccio
Jas Roux
Sample C
Sample A
Sample B
Routhierite
Arsiccioite
Stalderite
Ralphcannonite
Hg/(Hg+Zn+Fe)at.
Ag/(Ag+Cu)at.
0
0.1
0.2
0.3
0.4
0.5
0.6
0.7
0.8
0.9
1